Machine learning for mechanical properties classification in Additive Manufacturing

Paolo Di Giamberardino, Daniela Iacoviello
Dept. of Computer, Control and Management Engineering
Sapienza, University of Rome, Rome, Italy
paolo.digiamberardino@uniroma1.it, daniela.iacoviello@uniroma1.it

Filippo Berto, Rossella Fiorillo, Stefano Natali, Daniela Pilone, Carolina Schillaci
Dept. of Ingegneria Chimica Materiali Ambiente
Sapienza, University of Rome, Rome, Italy
rossella.fiorillo@uniroma1.it, daniela.pilone@uniroma1.it

Costanzo Bellini, Vittorio Di Cocco
Dept. of Dipartimento: Ingegneria Civile e Meccanica
Università degli Studi di Cassino e del Lazio Meridionale, Cassino, Italy
v.dicocco@unicas.it, c.bellini@unicas.it

***Abstract*—In the present paper, the effectiveness of the use of Machine Learning techniques, in particular Deep Learning algorithms, in the analysis of Ti-6Al-4V (Ti64) manufacture is studied; relationships between the values of physical parameters used during the production and mechanical characteristics are defined by means of the analysis of images taken from sections of the specimens, where defects and microstructural discontinuities can be observed. The Deep Learning approach, widely used for image classification and features extraction, also in this case shows promising possibilities, as proved by the implementation results reported.**

***Index Terms*—artificial intelligence, deep learning, additive manufacturing, Ti-6Al-4V alloy, mechanical properties, classification**

I. Introduction

Ti-6Al-4V (Ti64) is one the most versatile alloys, due to its biocompatibility, corrosion resistance, and high fracture toughness [1], [2]. These reasons make Ti64 particularly attractive across various fields, such as aerospace, automotive and biomedical, all requiring components that are usually complex in shape and lightweight [3]. The same needs are encouraging industries to increasingly adopt additive manufacturing (AM) techniques. These are widely used because of their flexibility in producing elaborate three-dimensional geometries without complex tools. Unlike traditional subtractive manufacturing methods, AM involves the deposition of subsequent layers of material during the fabrication of the components. However, AM components, as those produced through traditional methods, must meet the mechanical requirements of different industrial applications.

Defects and microstructural discontinuities are the main causes of the reduced static and fatigue life of AM components: this highlights the importance of controlling and preventing their formation [4]. However, the challenge lies in the fact that the development of defects, as well as residual stresses, microstructure, and distortion, depends on the set of selected production process parameters: during the manufacturing process, components are exposed to a complex thermal history, driven by rapid heating and cooling cycles [3], [4]. Among the defects of AM parts, lack of fusion, gas pores, keyhole porosities and high surface roughness are the most common ones, [5].

The defects due to lack of fusion are a kind of porosity caused by an insufficient energy input brought to the powder bed and have coarse geometries [6], while gas pores have a spherical or quasi spherical shape and are due to the presence of gas trapped in the material during the production process, [7].

On the other hand, if the electron beam power density is too high, metal vaporization occurs, generating recoil pressure that forms a cavity pushing the metal away from the molten zone, [8], [9]. If the cooling rate in the upper region of the keyhole is higher than in its base, pores are created due to keyhole collapse, [8], [9]. Based on these considerations, it is clear that the AM process parameters, influencing defect and microstructure formation, play a crucial role in determining the alloy's mechanical behavior. These considerations bring to the observation that a possible alternative to the direct measurement of the mechanical characteristics is to predict them considering the type and amounts of possible defects present in the sample. Moreover, being the defects strongly dependent on the physical parameters assumed during the fabrication stage, it is possible to assume the existence of one-to-one relationships between mechanical characteristics, defects in the samples and production processes. Then, the

possibility of analyzing the defects can bring to a fast, cheap and safe way to associate production process and mechanical characteristics.

In this work, the defect analysis is faced by making use of Machine Learning (ML) approaches, able to classify the defects by means of section images [10]. In particular, among the ML techniques, Deep Learning (DL) solutions have demonstrated a high efficiency for image analysis and feature recognition in a variety of applicative fields [10]–[15]. The availability of software tools and packages implementing in efficient ways ML algorithms has contributed to spread up this kind of approaches, with promising results. The present contribution follows these development lines and has the aim of proving that ML can give satisfactory results also in metallurgical areas. Then, Matlab® tools are here used for training a deep neural network for the classification of production samples through the defects' recognition.

The paper reports the problem definition in Section II, to clarify context and methodologies. Then, the metallurgical aspects are faced in Section III, illustrating the relationships between the problem posed and the information required for the subsequent phase of ML implementation, whose description is outlined in Section IV and implemented as described in Subsection IV-A. Some concluding discussion points and final comments in Section V end the paper.

II. Problem Definition

EBM is an AM technology that consists in melting metal powders in selected zones of a layer and repeating this operation layer by layer until the full sample is obtained. The energy source for such melting process is an electron beam, whose characteristics influence the microstructure of the produced parts. As a consequence, the microstructure of Ti6Al4V alloys produced via EBM is not significantly influenced by process parameters but contributes to the anisotropic behaviour of the alloy, [16]. On the other hand, production process parameters influence defect formation, which in turn affects the mechanical properties of the alloy.

Defects produced during the EBM process can be classified into three main categories: geometry-related defects, surface integrity defects, and microstructural defects, [17]. Geometry related defects arise from deviations between the CAD model and the size of the manufactured part. Surface integrity related defects refer to irregular surface features that deviate from the CAD model. This category includes defects such as the staircase effect, partially melted powders, balling effect, and surface cracking. Microstructural defects are internal imperfections that include hot and solid-state cracks, lack of fusion pores, keyhole pores, shrinkage cavities and textured columnar grains. These defects have a direct effect on the mechanical behaviour of the manufactured part and are influenced by production process parameters such as source power and scanning velocity.

Establishing a correlation between process parameters and defect size, orientation, and morphology is crucial. The size and morphology of discontinuities significantly influence the mechanical behaviour of the alloy under both static and dynamic conditions, as they affect stress concentration. The primary goal of this work is to develop a design tool that establishes a direct correlation between the process parameters used in EBM and the mechanical properties of the alloy, allowing better control of the production of material with higher performances. To this aim, as illustrated in the Introduction, the analysis of the defects, cheaper, faster and minimally invasive with respect to direct performances measurements on the samples, seems a promising approach to the optimization of production as well as to the process control for quality assurance.

Defects can be observed by visual inspection of sections of the sample, directly or by means of pictures. The image based analysis for defect detection and classification, required for solving the present problem, has led to the possibility of using Artificial Intelligent (AI) approaches, more specifically deep learning based modelling, as possible analysis techniques.

In the sequel, the whole machine learning approach is described, from the data set construction to the neural network training procedure till the check of effective possible use for defect detection and classification.

III. Additive Manufacturing Procedure for Data Set Definition

The first step in the present study has been the production of cylindrical specimens through the EBM process. The cylinders have a length of 135 mm and a diameter of 10 mm. To analyse the effect of process parameters, four different combinations of beam current and beam speed were selected, as reported in Table I. The beam current is representative of the quantity of electrons flowing in the beam, while the beam speed is the speed at which the beam spot moves across the powder layer surface. Along with the other parameters described below, they determine the quantity of energy the processed powder material receives. Regarding the other process parameters, their value was kept constant throughout the experimental campaign. The hatch distance between two adjacent beam scan tracks was set to 0.1 mm, while the thickness of each layer has been chosen equal to 50 μm. The current employed to regulate the electromagnetic lenses necessary for beam focusing, the focus offset current, has been set to 3 mA, with a beam generation voltage of 60 kV. Moreover, cylindrical specimens have been built with their axis both parallel and orthogonal to the building direction for each parameter set. Considering three repetitions for each set of parameters, a total of 24 specimens have been produced.

TABLE I
Parameters employed for the manufacturing of specimens.

Set	v, mm/s	I, mA
A	4530	15
B	6000	8
C	10000	15
D	9600	9

The machine used for parts production was the Arcam A2X, an EBM printer with a building envelope of $210 \times 210 \times$

380 mm^3. The manufacturing process started with the virtual placement of the cylindrical specimens in the machine building chamber using Magics Materialise software. In the same step, wafer support structures have been added to the specimens to reduce the warping and curling of the samples and, at the same time, to improve the heat dissipation. Then, the Materialise Build Processor software was used to slice the specimens' model, and the obtained data were transferred to the printing machine. The EBM control 3.2 was adopted to set the process parameters described above. After having filled the machine hopper with Ti6Al4V powder and closed the manufacturing chamber, the vacuum was generated inside.

When the warm-up temperature was reached, the first layer of powder was laid and selectively melted and, iteratively, all the subsequent layers were processed in a similar way. At the end of the stack production, the chamber was cooled down in a controlled manner till room temperature, the mass of unmelted powder with specimens inside was removed from the chamber, and the specimens were extracted from the powder. After having been cleaned using a high-pressure air chamber and an ultrasound bath, the cylinders were machined to obtain the dog-bone specimens like the one in Figure 1.

Fig. 1. One of the specimens obtained.

The specimen dimensions are evidenced in Figure 2. These dimensions have been chosen according to ASTM E8, the standard test method for evaluating the tensile properties of metal materials. It is worth noting that one specimen head is longer than the other one: samples for microstructure analysis have been extracted from there.

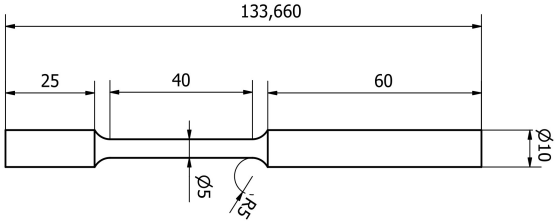

Fig. 2. Geometrical details for the produced specimens.

The set of images used for the subsequent phase of learning have then been generated using one sample for each set of parameters according to Table I, with two directions of cut, transversal with respect to the cylinders axis, i.e. vertical (A, B, C and D) and longitudinal, i.e. horizontal (AH, BH, CH and DH respectively). Examples of the images so obtained are depicted in Figures 3–6.

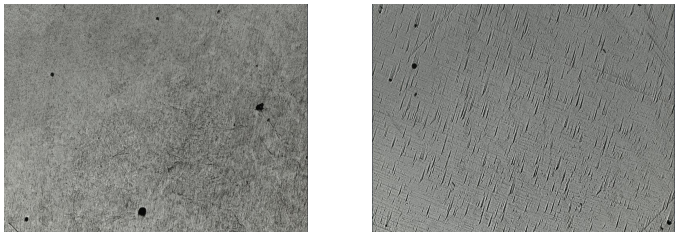

Fig. 3. First specimen: transversal (A, left) and longitudinal (AH, right) cut

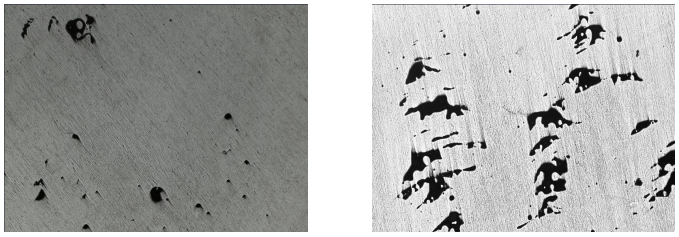

Fig. 4. Second specimen: transversal (B, left) and longitudinal (BH, right) cut

From each sample, 20 or 21 different sections are considered, depending on the mechanical cut. So, the initial Data Set is composed by 8 groups of 20 or 21 images; the identification system is required to be able to classify any further image as belonging to one of the eight group so that the physical parameter of construction and the mechanical properties of the sample can be associated.

IV. The Machine Learning Approach

The adoption of Artificial Intelligence (AI) based approaches to solve the above described problem is based on capabilities of such a technique to handle complex processes; they put in evidence, after a proper training phase, the relationships between the characteristics of the constructive materials,

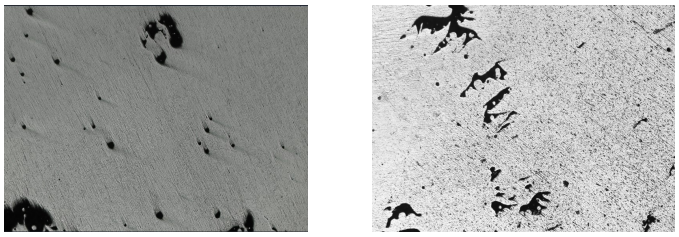

Fig. 5. Third specimen: transversal (C, left) and longitudinal (CH, right) cut

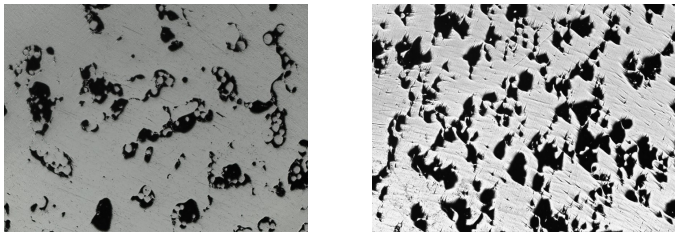

Fig. 6. Fourth specimen: transversal (D, left) and longitudinal (DH, right) cut

given by the Data Set images of the alloys surfaces, and the mechanical performances of the products, obtained after experimental tests. The use of such models as predictors would allow optimisation of the choice of controllable parameters in the fabrication phases, affecting the material defective state and the quality of the results on the basis of the characteristics of the starting pieces and the condition of the powders used and, therefore, the structure of the material, [18]. On the other hand, fast automatic detection of mechanical and structural characteristics of alloys, produced with additive manufacturing approaches under different physical construction conditions, can reduce the test and validation phases, allowing to ship expensive and time consuming direct measurements.

A deep learning approaches is here proposed, based on its ability to select and classify, by means of self–identified unlabelled features extraction, the corresponding mechanical and physic properties. A neural network, with a relevant number of inner hidden layers, in addition to the input and output ones, is trained using a sufficiently large amounts of data, the Data Set illustrated in Section III. Each inner layer implements a specific function, like segmentations and correlations, which are more deeply described in the implementation Subsection IV-A. Each additional hidden layer can help to better optimise and refine accuracy. The learning phase is carried out through multi parameters optimization schemes, like the processes of gradient descent, so that a deep learning algorithm can reach an accuracy sufficient to make predictions on a new photo with increased precision. This approach has already shown its potentialities in material characteristics analysis, [19]–[22].

A. The ML implementation

The AI model here developed, based on a deep learning algorithm, has been obtained making use of Matlab® and related Toolboxes; this choice has been supported by the observation that Automatic Image Classification with Convolutional Neural Networks (CNN) in MATLAB Machine Learning (ML) techniques are currently used for analysing large datasets in various fields; in particular, deep learning, an advanced ML technique, is effective for automatic image recognition, thanks to the richness and complexity of its structure. In fact, more in general, among the fundamental capabilities of deep learning, classification tasks are the most promising and most effective in different fields [13]–[15] and it represents a type of supervised learning in which a system learns how to classify new observations based on labelled data.

Here, the data are represented by the images obtained according to the description given in Section III for metal samples of Ti6Al4V alloy. In this first analysis, the samples are obtained using four different sets of physical characteristics, and each sample has been reported in the images after sectioning along two different orthogonal axes, longitudinal and transversal with respect to the direction of construction. So, there are eight classes to be identified, whose images are exampled in Figures 3–6. The eight classes have been named A, B, C, and D, for the four specimens with transversal cut for picture acquisition, and AH, BH, CH, and DH for the same specimens with horizontal cut.

So, a Convolutional Neural Network (CNN) has been chosen for the automatic classification of the micrograph images of metal samples. CNNs contain numerous layers: each of them is trained to be able to detect specific features from input images by applying filters, with different resolution for capturing specific characteristics of the images, and operations like convolutions or correlations. The sequential connections of the layers make the output of each processed image the input for the next layer. To proceed with the classification, a pre-trained residual network available in Matlab, ResNet18, consisting of 18 layers of depth, has been selected. The use of pre-trained models is a widely used approach when deep learning techniques are used [11], [12]. This network has a very powerful deep learning architecture, pre-trained on over a million images and capable of recognizing 1000 classes, [23]. ResNet18 has an input image size of 224×224 pixels with 3 channels (RGB, color images).

As previously described, the initial data set is composed by 165 images equally distributed among the 8 classes. For the deep learning approach, implemented by the ResNet18 network, 165 images constitute a poor data set with too limited number of original images: they are not sufficient for and effective network training. Moreover, at least 3 images for each class are excluded from the training and test procedures, to perform a final offline test. A possible solution to the lack of images is to increase their number by generating new images through transformations that do not introduce features deformations. This technique is often adopted; Matlab offers one data-augmentation function able to generate new images after various transformations to the datastore, arbitrarily defined: random rotation [-40°, +40°], translation [-30, +30] pixels, scaling [0.7, 1.3] and reflections. In our application, after this pre-processing phase on the data set, from the starting 141 original images 564 augmented images are obtained, collected in subfolders corresponding to the original classes.

The final pre-processing operation involved resizing all input images, originally sized at 1024×1536 pixels, to match the 224×224 pixel input size required by ResNet18. Going deeply in the training algorithm, ResNet18 consists of an input layer that receives the resized 224×224 pixel images, an output layer that returns the classes, and multiple hidden layers in between. These are convolutional blocks that extract features from the images and establish connections between them.

The final three layers are:

- the fully connected layer, *fc1000*, which processes the extracted features and passes them through the ReLU activation function to improve the model's ability to distinguish classes;
- the softmax layer, *prob*, which defines the probability of each image belonging to a specific class;
- the Classification Output layer, *ClassificationLayers_predictions*, which displays the predicted class.

This architecture has been then customized to fit the specific problem: the *fc1000* layer has been replaced with a new one, *fc_new*, to output 8 classes and the *prob* and *Classification-Layers_predictions* layers have been updated, *softmax_new* and *classOutput*, respectively, to support the present 8 classes instead of the original 1000.

So, the training phase has been carried on making use of the datastore containing the augmented images organized by class. According to the most usual choices, the augmented datastore was randomly divided into three subsets: 70% as training data, 15% as validation data and 15% for test.

The structured model was trained using the following settings: Adam optimization algorithm with an initial learning rate of 0.001, 5 epochs and a mini-batch size of 11.

These options have been defined after a few training trials to achieve an accuracy of around 90% with an approximate training time of ten minutes. During training, the network was monitored through the progress graph, which visualized the training process and the loss-function, providing an immediate feedback. The final graphs for accuracy and loss during the learning epoch is reported in Figure 7.

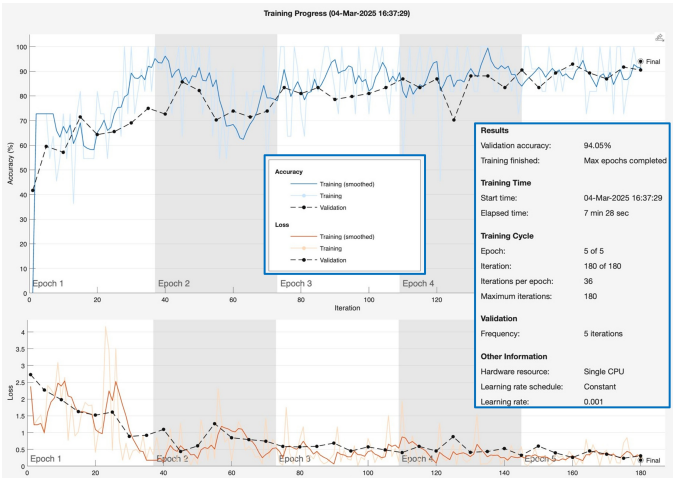

Fig. 7. Representation of the training progress in the first case

The validation phase occurs simultaneously with the training one. The training has been repeated to ensure no over-fitting and guarantee that the validation accuracy remains stable (between 88% and 96%).

Upon completing the training, the model has been tested on the test dataset, achieving an accuracy between 88% and 98%. The confusion matrix reported in Figure 8 was also generated to visualize the distribution of correct and incorrect classifications. It is possible to highlight challenges in distinguishing visually similar classes, such as A, B, C, and BH, CH, as seen in Figures 3–6. A deeper analysis has been performed, and some comments are reported in the next Section V: misclassification has been further analyzed by examining the erroneously classified images to identify patterns to be improved to avoid confusion.

As a final quality check, the trained model has been finally applied to the 24 images initially excluded from the datastore

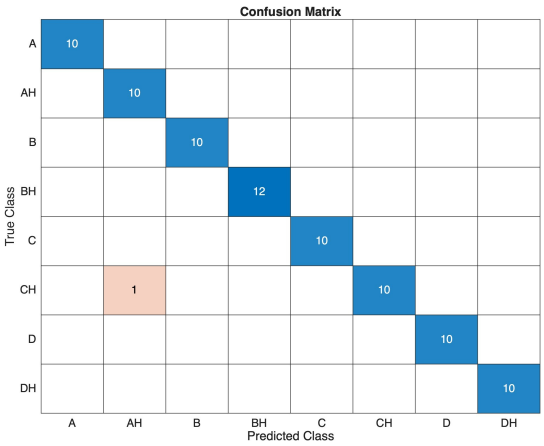

Fig. 8. Resulting confusion matrix for the first training case

during the initial phase, so that they are totally new and unknown to the network. The classification process has shown promising results, with 96% of the images correctly identified by class (it means only one wrong answer).

For further verification, the data augmentation technique has been also applied to the test images generating 96 additional augmented images. In this case, the classification yields correct results for 91% of the images.

Training progress and confusion matrix for this case are reported in Figures 9 and 10 respectively.

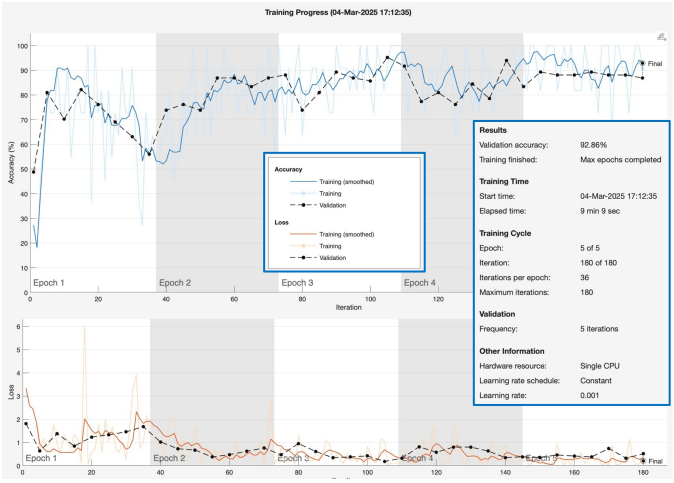

Fig. 9. Representation of the training progress in the second case

V. Results and Conclusions

In this study, samples made of Ti-6Al-4V (Ti64) alloy have been produced using various process parameters, to investigate their influence on defect formation within the material and, consequently, on the mechanical characteristic of the sample.

The analysis has been performed by means of Deep Learning algorithms, whose application to the pictures of specimens' sections has shown high potentiality, efficacy and effectiveness perspective in the classes' recognition and classification.

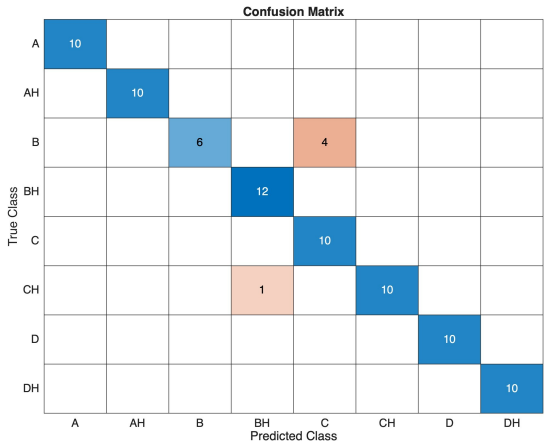

Fig. 10. Resulting confusion matrix for the second training case

In particular, in the results presented above, it can be observed that the images that are most frequently confused are those showing transversal with respect to the sample axis, where visually distinguishing the differences in defects is difficult. However, sections with a high number of defects (D) are never confused with the others. The classification of the excluded images also confirms these results. These results confirm the robustness of the model in recognizing the 8 classes of Ti6Al4V samples. However, opportunities for improvement remain, such as refining the training options or exploring alternative architectures.

Another consideration could be the augmented images, which are variations of the original images; therefore, if the algorithm were repeated with a larger initial dataset, it would provide further validation of the model's robustness in recognizing the specified classes. Even for the present low dimension of the training data set, the performances of the classification system are significantly high. The perspective of future implementation with a larger set of images and with a greater number of classes is very promising.

ACKNOWLEDGMENTS

This work has been partially supported by PRIN grant *I-ADMA Mechanical behaviour prediction of ADditively MAnufactured component by an artificial Intelligence approach* from Italian MIUR.

REFERENCES

[1] H. Galarraga, D. A. Lados, R. R. Dehoff, M. M. Kirka, and P. Nandwana, "Effects of the microstructure and porosity on properties of Ti-6Al-4V ELI alloy fabricated by electron beam melting (EBM)," *Addit Manuf*, vol. 10, pp. 45–57, 2016.

[2] S. Liu and Y. C. Shin, "Additive manufacturing of Ti6Al4V alloy: A review," *Mater Des*, vol. 164, 2019.

[3] A. Gupta, C. J. Bennett, and W. Sun, "The role of defects and characterisation of tensile behaviour of EBM additive manufactured Ti-6Al-4V: An experimental study at elevated temperature," *Eng Fail Anal*, vol. 120, 2021.

[4] M. C. Brennan, J. S. Keist, and T. A. Palmer, "Defects in metal additive manufacturing processes," *J. Mater Eng Perform*, vol. 30, no. 7, pp. 4808—-4818, 2021.

[5] N. Shamsaei, A. Yadollahi, L. Bian, and S. M. Thompson, "An overview of direct laser deposition for additive manufacturing; part ii: Mechanical behavior, process parameter optimization and control," *Elsevier B.V.*, 2015.

[6] T. D. Terris, T. Baffie, and C. Ribière, "Additive manufacturing of pure copper: a review and comparison of physical, microstructural, and mechanical properties of samples manufactured with laser-powder bed fusion (l-pbf), electron beam melting (ebm) and metal fused deposition modelling (mfdm) technologies," *International Journal of Material Forming*, vol. 16, no. 4, 2023.

[7] T. Kurzynowski, M. Madeja, R. Dziedzic, and K. Kobiela, "The effect of EBM process parameters on porosity and microstructure of Ti-5Al-5Mo-5V-1Cr-1Fe alloy," *Scanning*, vol. 2019, 2019.

[8] Y. Chen, S. J. Clark, C. L. A. Leung, L. Sinclair, S. Marussi, M. P. Olbinado, E. Boller, A. Rack, I. Todd, and P. D. Lee, "In-situ synchrotron imaging of keyhole mode multi-layer laser powder bed fusion additive manufacturing," *Applied Materials Today*, vol. 20, p. 100650, 2020.

[9] M. Qu, Q. Guo, L. I. Escano, S. J. Clark, K. Fezzaa, and L. Chen, "Mitigating keyhole pore formation by nanoparticles during laser powder bed fusion additive manufacturing," *Additive Manufacturing Letters*, vol. 3, p. 100068, 2022.

[10] V. B. Shalini, B. Kumar, P. V. Varma, P. V. K. Reddy, and T. T. Kumar, "Machine learning based leaf disease diagnosis system," *2025 International Conference on Multi-Agent Systems for Collaborative Intelligence (ICMSCI)*, pp. 1124–1128, 2025.

[11] A. Blaze Pitta, N. Reddy Pingala, M. Charan Jaladhi, Naga Venkata, S. Bogolu, and B. Suvarna, "Footwear classification using pretrained cnn models with deep neural network," in *2025 International Conference on Multi-Agent Systems for Collaborative Intelligence (ICMSCI)*, pp. 1729–1736, 2025.

[12] D. Marmanis, M. Datcu, T. Esch, and U. Stilla, "Deep learning earth observation classification using imagenet pretrained networks," *IEEE Geoscience and Remote Sensing Letters*, vol. 13, no. 1, pp. 105–109, 2016.

[13] S.-J. Liu, H. Luo, and Q. Shi, "Active ensemble deep learning for polarimetric synthetic aperture radar image classification," *IEEE Geoscience and Remote Sensing Letters*, vol. 18, no. 9, pp. 1580–1584, 2021.

[14] K. Muhammad, S. Khan, J. D. Ser, and V. H. C. d. Albuquerque, "Deep learning for multigrade brain tumor classification in smart healthcare systems: A prospective survey," *IEEE Transactions on Neural Networks and Learning Systems*, vol. 32, no. 2, pp. 507–522, 2021.

[15] B. Kim, T. S. Mathai, K. Helm, P. A. Pinto, and R. M. Summers, "Classification of multi-parametric body mri series using deep learning," *IEEE Journal of Biomedical and Health Informatics*, vol. 28, no. 11, pp. 6791–6802, 2024.

[16] H. K. Rafi, N. V. Karthik, H. Gong, T. L. Starr, and B. E. Stucker, "Microstructures and mechanical properties of ti6al4v parts fabricated by selective laser melting and electron beam melting," *J. of Materi Eng and Perform*, vol. 22, pp. 3872—-3883, 2013.

[17] J. Fu, H. Li, X. Song, and M. Fu, "Multi-scale defects in powder-based additively manufactured metals and alloys," *Journal of Materials Science & Technology*, vol. 122, pp. 165–199, 2022.

[18] V. V. Popov, A. Katz-Demyanetz, A. Garkun, and M. Bamberger, "The effect of powder recycling on the mechanical properties and microstructure of electron beam melted Ti-6Al-4V specimens," *Additive Manufacturing*, vol. 22, pp. 834–843, 2018.

[19] N. Johnson, P. Vulimiri, A. To, X. Zhang, C. Brice, B. Kappes, and A. Stebner, "Invited review: Machine learning for materials developments in metals additive manufacturing," *Additive Manufacturing*, vol. 36, 2020.

[20] J. Chen and Y. Liu, "Fatigue modeling using neural networks: A comprehensive review," *Fatigue and Fracture of Engineering Materials and Structures*, vol. 45, no. 4, pp. 945–979, 2022.

[21] H. Kollmann, D. Abueidda, S. Koric, E. Guleryuz, and N. Sobh, "Deep learning for topology optimization of 2d metamaterials," *Materials and Design*, vol. 196, 2020.

[22] T. Ni, B. Guo, and C. Yang, "Design of ultrasonic testing system for defects of composite material bonding structure based on deep learning technology," *2020 International Conference on Virtual Reality and Intelligent Systems*, pp. 263–266, 2020.

[23] *https://it.mathworks.com/discovery/neural-network.html*, 2025.